

LETTER TO THE EDITOR

Generation of rotationally dominated galaxies by mergers of pressure-supported progenitors

Paola Di Matteo¹, Chanda J. Jog², Matthew D. Lehnert¹, Françoise Combes³, Benoit Semelin³

¹ Observatoire de Paris, section de Meudon, GEPI, 5 Place Jules Janssen, 92195, Meudon, France

² Department of Physics, Indian Institute of Science, Bangalore 560012, India

³ Observatoire de Paris, LERMA, 61 Avenue de l'Observatoire, 75014 Paris, France

Accepted, Received

ABSTRACT

Through the analysis of a set of numerical simulations of major mergers between initially non-rotating, pressure supported progenitor galaxies with a range of central mass concentrations, we have shown that: (1) it is possible to generate elliptical-like galaxies, with $v/\sigma > 1$ outside one effective radius, as a result of the conversion of orbital- into internal-angular momentum; (2) the outer regions acquire part of the angular momentum first; (3) both the baryonic and the dark matter components of the remnant galaxy acquire part of the angular momentum, the relative fractions depend on the initial concentration of the merging galaxies. For this conversion to occur the initial baryonic component must be sufficiently dense and/or the encounter should take place on a orbit with high angular momentum. Systems with these hybrid properties have been recently observed through a combination of stellar absorption lines and planetary nebulae for kinematic studies of early-type galaxies. Our results are in qualitative agreement with such observations and demonstrate that even mergers composed of non-rotating, pressure-supported progenitor galaxies can produce early-type galaxies with significant rotation at large radii.

Key words. galaxies: interaction – galaxies: formation – galaxies: evolution – galaxies: structure and kinematics

1. Introduction

It has been known for several decades that early type galaxies have complex kinematics and varying amounts of rotation and that these characteristics depend on luminosity and isophotal shape (e.g., Davies 1983; Bender 1988). Recently, the results of the SAURON survey (Bacon et al. 2001; de Zeeuw et al. 2002) have lead to a division of early-type galaxies into two distinct classes, slow and fast rotators, depending on the amount of the angular momentum per unit mass of their stellar component inside one effective radius (R_e ; Emsellem et al. 2007). These two classes also have different properties, slow rotators are generally more massive, less flattened systems than fast rotators (Cappellari et al. 2007). Studies of the more distant regions of early-type galaxies, traced by planetary nebulae, have shown that their complexity of the kinematics of the inner regions also extends to the outer halos (Coccatto et al. 2009). Interestingly, these outer haloes can be more rotationally dominated than their central regions (Coccatto et al. 2009).

Extensive studies using numerical simulations suggest that different processes lead to the formation of slow and fast rotating early-type galaxies. Most of these studies have focused on the remnants of spiral-spiral mergers, which is likely to be an important process for the evolution of formation of ellipticals and perhaps responsible for driving galaxies from the blue cloud to the red sequence (Cattaneo et al. 2006; Faber et al. 2007; Romeo et al. 2008). Even if the agreement between simulations and observations is often qualitative only - which is most likely due to incomplete knowledge of the characteristics of the progenitors of these merger remnants - some conclusions can still be drawn (Quinn et al. 1993; Naab et al. 1999; Velazquez & White 1999; Bendo & Barnes

2000; Cretton et al. 2001; Naab & Burkert 2003; Bournaud et al. 2004, 2005; Naab et al. 2006a; González-García & Balcells 2005; González-García et al. 2006; Jesseit et al. 2007, 2008). Mergers of two spirals can produce rotationally supported early-type galaxies (at radii inside $1 R_e$), depending on the mass ratio of the progenitors. Major mergers (1:1 mass ratio) are sufficiently violent to completely destroy the initial ordered rotational motions in the progenitor disks¹, typically producing a pressure-supported system. Apparently, mergers with higher mass ratios can generally produce remnants with significant rotation. Virtually all the focus so far has been on simulated spiral-spiral interactions, attempting to answer to the question: Is it possible to (at least partially) preserve the initial internal angular momentum of the progenitor disks?

Encounters between pressure supported (spheroid dominated) galaxies have been systematically studied by White (1978, 1979); González-García & van Albada (2005a,b); González-García et al. (2006). These studies show that such mergers result in a wide variety of remnant properties. In particular, González-García & van Albada (2005a) pointed out that mergers of spherically symmetric galaxies, without dark matter, can result in remnants partially supported by rotation and that part of the orbital angular momentum is absorbed by the halo, when present (González-García & van Albada 2005b). However, none of these studies have investigated in detail how the orbital angular momentum is redistributed during the

¹ Unless peculiar configurations are considered (Pfenniger 1997; Puerari & Pfenniger 2001) or the amount of gas in the progenitor disks is sufficiently high (Springel & Hernquist 2005; Robertson et al. 2006; Hopkins et al. 2009).

interaction, nor have they investigated the dynamical properties of the remnants out to large distances (several R_e).

In this Letter, we show, for the first time, that mergers of initially spherical, pressure-supported stellar systems without rotation can produce hybrid remnants having elliptical-like morphology, but are dominated by rotation ($v/\sigma > 1$). As we shall demonstrate, the final characteristics of the remnant depends on both the initial orbital angular momentum and the central density of the merging galaxies.

2. Models and initial conditions

We study the coalescence of two equal-mass elliptical galaxies, consisting of a stellar and a dark matter (DM) component, distributed in a Plummer density profile, without any dissipational component and initial rotation. The density profile of the dark matter halo is the same in all the simulations, we only changed the central density of the baryonic component in order to study how changing the density affects the angular momentum (AM) redistribution during the encounter. We thus considered gE0, gE0 and gE0m models, with increasing central stellar density (Table 1 and Fig. 1), whose half-mass radii r_{50} and effective densities σ^2/r_{50}^2 are in agreement with observational estimates for galaxies with $M_r = -22$ (Desroches et al. 2007), assuming a $M/L=3$ in the r-band. Since the total mass of the stellar component is fixed, increasing the central stellar density results in a more concentrated and compact stellar profile. In these models, the DM contributes ~ 10 -30% of the total mass within the half-mass radius of the baryonic component, in agreement with observational estimates (Barnabe et al. 2009). The initial galaxies have been then placed at a relative distance of 100 kpc, with a variety of relative velocities, in order to simulate different orbits (orbital energies and angular momenta; see Di Matteo et al. (2009)). In particular, in the following we will show results from three of these orbits (id=01, 05, 15), whose main parameters are given in Table 2. When referring to specific encounters, the nomenclature adopted is the following: morphological type of the two galaxies in the interaction (gE0, gE01 or gE0m), plus the encounter identification string (see first column in Table 2). Each pair has been modeled with $N = 120000$ particles, distributed among stars ($N_{star} = 80000$) and dark matter ($N_{DM}=40000$).

All the simulations have been run using the Tree-SPH code described in Semelin & Combes (2002). A Plummer potential is used to soften the gravity at small scales, with constant softening lengths of $\epsilon = 280$ pc for all particles. The equations of motion are integrated using a leapfrog algorithm with a fixed time step of 0.5 Myr. With these choices, the relative error in the conservation of the total energy is of the order of 2×10^{-7} per time step. Since the work presented here only investigates dry-mergers, only the part of the code evaluating the gravitational forces acting on the systems has been used.

3. Results

3.1. Angular momentum redistribution: dependence on the orbits

The first question we would like to address is: how orbital AM is redistributed and converted into internal AM during an interaction and how does this depend on the orbital parameters of the encounter? In Fig. 2, we show the evolution of the total, orbital and internal AM, for two different orbits (id=15 and id=05), corresponding, respectively, to increasing initial orbital angular momenta. The AM is evaluated with respect to the barycenters of

the two galaxies, considering all the particles. The main results are:

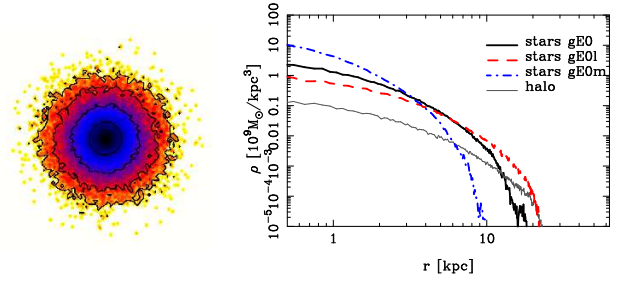


Fig. 1. Initial properties of the galaxy models: (a) projected density map of the stellar component of the gE0 galaxy; (b) volume-density profiles of the galaxy models. The model is as indicated in the legend of the figure.

Table 1. Parameters for the standard (gE0), less concentrated (gE01) and more concentrated (gE0m) model galaxies. Both the stellar and dark matter profiles are represented by Plummer models, having characteristic masses, respectively, given by M_B and M_H for the baryons and halo respectively, and core radii given by r_B and r_H for the baryons and halo respectively. The initial half-mass radii r_{50} of the baryonic component and effective densities σ^2/r_{50}^2 are also given.

	M_B, M_H [$2.3 \times 10^9 M_\odot$]	r_B, r_H [kpc]	r_{50} [kpc]	$\log(\sigma^2/r_{50}^2)$ [(km/s/kpc) 2]
gE0	70, 30	4.0, 7.0	5.2	3.2
gE01	70, 30	6.0, 7.0	7.5	2.9
gE0m	70, 30	2.0, 7.0	2.8	3.9

Table 2. Orbital parameters

orbit id	r_{ini}^a [kpc]	v_{ini}^b [100 km s^{-1}]	L^c [$10^2 \text{ km s}^{-1} \text{ kpc}$]	E^d [$10^4 \text{ km}^2 \text{ s}^{-2}$]
01	100.	2.0	57.0	0.
05	100.	2.0	80.0 ^e	0.
15	70.0	1.6	41.3	-1.57

^a The initial distance between the two galaxies.

^b The absolute value of the initial relative velocity between the two galaxies.

^c The absolute value of the orbital angular momentum of the unit mass, i.e., $L = |\mathbf{r}_{ini} \times \mathbf{v}_{ini}|$.

^d The total energy of the relative motion, i.e., $E = v_{ini}^2/2 - G(m_1 + m_2)/r_{ini}$, with $m_1 = m_2 = 2.3 \times 10^{11} M_\odot$.

^e Even if the initial relative velocities in orbit 05 and 01 are equal, their orbital angular momenta differ because the initial orbital tangential velocities are different.

- The total AM is (obviously) conserved during the interaction.
- The orbital AM is constant until the first pericenter passage between the two galaxies. When this happens, dynamical friction and tidal torques act efficiently on the systems, converting part of the orbital AM into internal AM.

- At every successive close passage between the two galaxies, part of the orbital AM is converted into internal rotation of the two systems. This process ends when all the orbital AM is converted into internal AM and the two galaxies finally merge.
- Instead of defining the merging time as the point when the two galaxy centres are sufficiently close we suggest, based on dynamical arguments, that the merging time could be the point when orbital AM is totally converted into internal AM (as we verified, these two definitions give similar merging times). This definition, of course, applies only for orbits having an initial orbital AM different from zero.
- Because of AM conservation, the final amount of internal AM of the remnant galaxy depends on the initial amount of orbital AM.

In Fig. 3, we show the evolution with time of the specific internal AM for both the stellar and the dark matter components. For each of the two galaxies, and for each component (baryons and halo), we evaluate the specific internal AM in four different radial regions. From this analysis, we can deduce that:

- *The orbital AM is converted into internal AM “outside-in”, the external regions acquire part of the angular momentum first.*
- Interestingly, between the first pericenter passage and the final phases of coalescence, the outer regions show some rotation, while the inner regions do not.
- Both the baryonic and the dark matter component acquire part of the orbital AM, and both the components, in the final remnant, show some rotation. *The two initially non-rotating and spherically symmetric components are thus transformed into a flattened rotating system*².
- The higher the initial orbital AM, the higher the internal specific AM of the final remnant, at all radii.

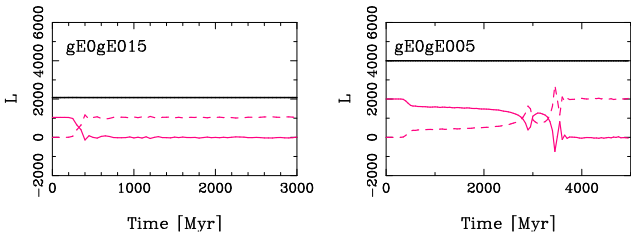


Fig. 2. Evolution of the total (black line), orbital (solid red line) and internal (dashed red line) AM for two different orbits. The two galaxies are identical, so the internal and orbital AM are shown only for one of the two. The angular momenta are all measured perpendicular to the orbital plane and are in units of $2.3 \times 10^{11} M_{\odot} \text{ kpc km s}^{-1}$.

3.2. Angular momentum redistribution: dependence on the galaxy central density

To investigate how the evolution and redistribution of AM depend on the initial central density of the two progenitors, we also simulated mergers with a range of concentrations (gE0l-gE0 - less concentrated and gE0m-gE0m - more concentrated).

² As we confirmed, the remnants show some velocity anisotropy and both rotation and anisotropy contribute to the flattening. A discussion on this will be presented in a more detailed paper.

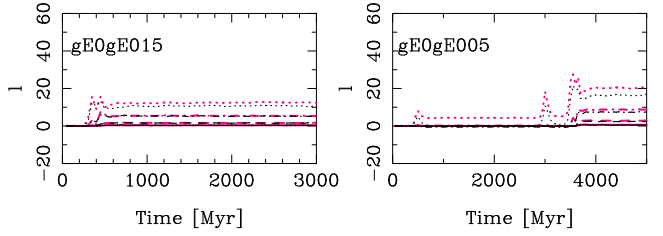


Fig. 3. Evolution of the specific AM, l , for four different regions of one of the two elliptical galaxies ($r \leq 2\text{kpc}$, solid lines, $2\text{kpc} < r \leq 5\text{kpc}$ dashed lines, $5\text{kpc} < r \leq 10\text{kpc}$, dot-dashed lines, and $10\text{kpc} < r \leq 20\text{kpc}$, dotted lines). The specific AM of the stellar component is shown in red, that of the dark matter component in gray. l is in units of $100 \text{ kpc km s}^{-1}$. In the two panels, the initial orbital parameters of the interaction has been varied, so to have an increasing orbital AM, going from left to right, while the morphology of the interacting galaxies has been kept fixed. The specific angular momenta are all measured perpendicular to the orbital plane.

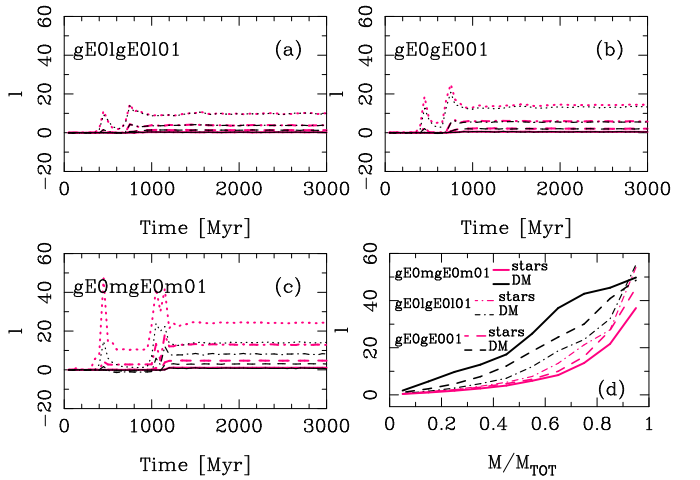


Fig. 4. Panels (a), (b) and (c) show results similar to Fig. 3, but now the panels show the evolution of the specific AM for interacting pairs having initially the same orbital parameters, but different morphologies (the stellar central densities increase from panel a-c). Panel (d): Specific AM, l , of the remnant galaxies as a function of radii containing a fixed percentage of the baryonic (red lines) and halo (black lines) mass. l has been evaluated at least 1 Gyr after the coalescence of the two progenitors. Line-styles correspond to the different morphologies shown in panels (a), (b) and (c), i.e., gE0lgE0l01 (dot-dashed line), gE0gE001 (dashed line), gE0mgE0m01 (solid line).

Fig. 4 shows the evolution with time of the specific internal AM for four different regions in the galaxy (see also Fig. 3). Since the initial orbital AM are the same in these simulations, the amount of internal AM of the final remnant will also be the same. However, AM is redistributed in a quite different way, depending on the initial concentration of the progenitor galaxies. We find that mergers with higher initial galaxy central density produce remnants with larger relative amount of rotation at any radius within a radius of 20 kpc. This result is true for both the baryonic and dark matter components.

This behavior is related to the fact that the three remnant galaxies have different mass distribution profiles, as we will discuss in the next Section, and so ultimately the physical regions chosen in Fig. 4 contain different amount of baryonic and dark

matter mass. A more appropriate comparison is the distribution of the specific AM within a constant fraction of the mass. We show the distribution of the specific AM as a function of radii containing a fixed percentage of the baryonic (red lines) or dark matter (black lines) mass in Fig. 4, panel (d). Again, this is evaluated at least 1 Gyr after the merger has completed. The internal rotation is distributed in a quite different way in the three remnants as a function of mass. The baryons in each of the models have a similar distribution of l inside the effective radius, while outside it, less concentrated progenitors lead to a higher amount of specific AM. The dark matter component, however, shows the opposite trend – the specific AM is higher for all values of the enclosed mass for progenitors with high concentration. This is because more concentrated baryonic components are less responsive to tidal torques, while the outer, less concentrated halo is more strongly affected by the tidal interaction. To illustrate this, in the case of the gE0lgE0l01 interaction, at the end of the simulation about 67% of the orbital AM has been acquired by the baryons, and only 33% by the dark halo, while for the most concentrated case (gE0mgE0m01) the two components have acquired similar percentage of the initial orbital AM (48% for the baryons and 52% for the halo).

Thus *baryonic components with low concentration are more susceptible to tidal torques, and thus acquire a higher percentage of the initial orbital angular momentum.*

3.3. Mergers of dense pressure-supported systems: rotationally-dominated systems with an elliptical-like morphology

The varying amount of specific AM found in remnants of progenitors having different initial concentrations is also reflected in the kinematics. A detailed analysis of the relationship between the morphological and dynamical properties of mergers of pressure-supported systems will be the topic of a future paper. Here we simply note that when a sufficient amount of specific AM is imparted to the central regions of the remnant galaxy, such remnants may show interesting hybrid properties. Some may have a morphology typical of an elliptical galaxy, but a v/σ ratio higher than 1, over most of their extended stellar distribution. This is the case, for example, in the gE0mgE0m01 merger remnant. Even if its baryonic component has a specific AM inside the half-mass radius similar to that of the less concentrated galaxies (panel d of Fig. 4), the gE0mgE0m01 remnant is much denser than, for example, the gE0lgE0l01 remnant (Fig. 5). The different mass distribution of the two galaxies is reflected in different dynamical properties in an interesting way: even if they acquire a lower percentage of the orbital AM, being less susceptible to tidal torques, the baryonic components of the most concentrated systems show a higher central velocity dispersion, a steeper dispersion profile, a higher value of the line-of-sight velocities, and a v/σ ratio which becomes greater than 1 at about $r = r_{50}$ (the baryonic half-mass radius; Fig. 6). This may appear paradoxical, but this is due to the fact that the internal AM is redistributed over a much more compact distribution compared to low-concentration remnants. Most of the galaxies studied by Coccato et al. (2009) show a v/σ ratio not greater than 0.6, while a fraction of them have kinematics that become increasingly supported by rotation in the outer parts, qualitatively in agreement with the hybrid merger remnants discussed here. This supports the idea that the morphological properties of a galaxy are not univocally related to the dynamical ones. Mergers can indeed produce hybrid systems, having a spiral-like morphology but an elliptical-like kinematics (Jog & Chitre 2002; Bournaud et al.

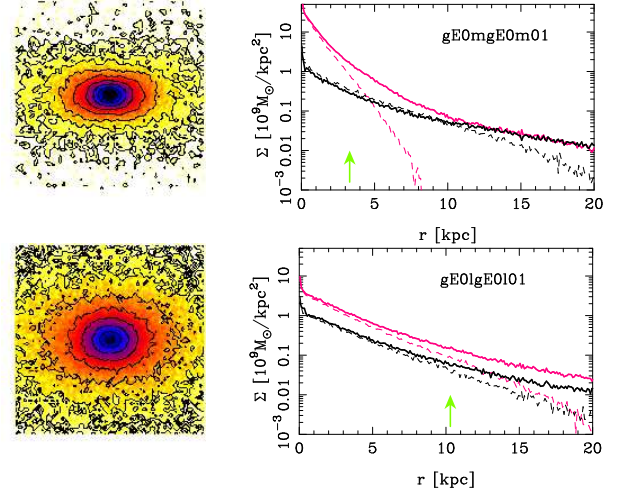


Fig. 5. Morphological characteristics of two remnants of pressure-supported, initially non-rotating galaxies. Top panels: (Left) Projected density map of the remnant of the gE0mgE0m01 encounter (progenitors with high concentrations); (right) Surface density profile of the baryonic (red color) and dark matter component (black color) of the remnant (solid line) and its progenitor galaxy (dashed line). The green arrows indicate the half mass radius (r_{50}) of the baryonic component. Bottom panels: Same as top panels, but progenitors with relatively low concentrations (gE0lgE0l01).

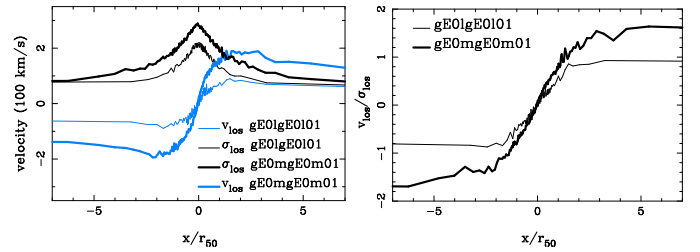


Fig. 6. Kinematical properties of two remnants of E-E mergers. Left panel: line-of-sight velocities (blue) and velocity dispersions (black) of the gE0mgE0m01 (thick lines) and of the gE0lgE0l01 (thin lines) remnants. Right panel: corresponding v/σ ratio (gE0mgE0m01, thick line; gE0lgE0l01; thin line).

2004, 2005) or, as presented here, elliptical-like morphology but are rotationally-dominated.

4. Conclusions

Through the analysis of a set of numerical simulations of major mergers between initially non-rotating, pressure supported progenitor galaxies, we have shown that it is possible to generate elliptical-like galaxies, with $v/\sigma > 1$ outside one effective radius, simply as a result of the conversion of the orbital AM into internal one, during the mergers of two initially non-rotating progenitors. For this to occur the initial baryonic component must be sufficiently dense and/or the encounter should take place on a high AM orbit.

Systems with such hybrid properties have been recently observed. For example, Coccato et al. (2009) found that galaxies in their sample with the most steeply declining velocity profiles have generally fast rotating halos, as found for our fast rotating remnants. Our results are in qualitative agreement with such observations and demonstrate that even mergers composed

of non-rotating, pressure-supported progenitor galaxies can produce early-type galaxies with significant rotation at large radii. In particular, we stress the important point that this mechanism does not require initially any internal AM in the colliding galaxies.

Simulations by Naab et al. (2006b) show that repeated binary early-type mergers lead to the formation of anisotropic, slowly rotating elliptical galaxies (inside R_e). In this context, whether the hybrid systems presented in this Letter can be formed frequently and maintained also after successive mergers should be studied with a larger set of simulations, taking into account repeated mergers (major and minor) with different relative inclinations, as well as progenitors with different DM profiles (Navarro et al. 1997).

Nevertheless, it is possible to hypothesize a scenario where these elliptical, rotationally-supported systems are mainly found among remnants of dense early-type galaxies. These hybrid features will tend to vanish if successive major mergers take place, with a random orientation of the internal and orbital AM with respect to the spin of the "hybrid" galaxy. But this has yet to be investigated numerically.

Acknowledgments

PDM was awarded a travel grant from the Indo-French Astronomy Network which made possible a visit to IISc, Bangalore, in November 2008. PDM is supported by a grant from the Agence Nationale de la Recherche (ANR) in France. We thank the referee for comments which helped to improve the paper.

References

- Bacon, R., Copin, Y., Monnet, G., Miller, B. W., Allington-Smith, J. R. et al. 2001, MNRAS, 326, 23
- Barnabe, M., Czoske, O., Koopmans, L., Treu, T., Bolton, A. et al. 2009, MNRAS, in press; astro-ph/0904.3861
- Bender, R. 1988, A&A, 193, L7
- Bendo, J. G. & Barnes, J. E. 2000, MNRAS, 316, 315
- Bournaud, F., Combes, F., Jog, C. J. 2004, A&A, 418, L27
- Bournaud, F., Jog, C. J., Combes, F. 2005, A&A, 438, 507
- Cappellari, M., Emsellem, E., Bacon, R., Bureau, M., Davies, R. L. et al. 2007, MNRAS, 379, 418
- Cattaneo, A., Dekel, A., Devriendt, J., Guiderdoni, B., Blaizot, J. 2006, MNRAS, 370, 1651
- Cocato, L., Gerhard, O., Arnaboldi, M., Das, P., Douglas, N. G. et al. 2009, MNRAS, 394, 1249
- Cretton, N., Naab, T., Rix, H.-W., & Burkert, A. 2001, ApJ, 597, 893
- Davies, R. L., Efstathiou, G., Fall, S. M., Illingworth, G., Schechter, P. L. 1983, ApJ, 41, 57
- de Zeeuw, P. T., Bureau, M., Emsellem, E., Bacon, R., Carollo, C. M., et al. 2002, MNRAS, 329, 513
- Desroches, L.-B., Quataert, E., Ma, C.-P., West, A. A. 2007, MNRAS, 377, 402
- Di Matteo, P., Pipino, A., Lehnert, M. D., Combes, F., Semelin, B., 2009, A&A, in press; astro-ph/0903.2846
- Emsellem, E., Cappellari, M., Krajnović, D., van de Ven, G., Bacon, R. et al. 2007, MNRAS, 379, 401
- González-García, A. C., Balcells, M., Olshevsjy, V. S. 2006, MNRAS, 372, L78
- González-García, A. C., & Balcells, M., 2005, MNRAS, 357, 753
- González-García, A. C., & van Albada, T. S. 2005a, MNRAS, 361, 1030
- González-García, A. C., & van Albada, T. S. 2005b, MNRAS, 361, 1043
- Hopkins, P. F., Cox, T. J., Younger, J. D., Hernquist, L. 2009, ApJ, 691, 1168
- Jesseit, R., Cappellari, M., Naab, T., Emsellem, E., Burkert, A. 2008, submitted to MNRAS; astro-ph/0810.0137
- Jesseit, R., Naab, T., Peletier, R. F., Burkert, A. 2007, MNRAS, 376, 997
- Jog, C. J. & Chitre, A. 2002, A&A, 393, L89
- Faber, S. M., Willmer, C. N. A., Wolf, C., Koo, D. C., Weiner, B. J. et al. 2007, ApJ, 665, 265
- Naab, T., Jesseit, R., Burkert, A. 2006a, MNRAS, 372, 839
- Naab, T., Khochfar, S., Burkert, A. 2006b, ApJ, 636, L81
- Naab, T. & Burkert, A. 2003, ApJ, 597, 893
- Naab, T., Burkert, A., Hernquist, L. 1999, ApJ, 523, L133
- Navarro, J. F., Frenck, C. S., White, S. D. M. 1997, ApJ, 490, 493
- Pfenniger, D. 1997, Contribution to IAU Symp. 186, Galaxy Interactions; astro-ph/9712022
- Puerari, I. & Pfenniger, D. 2001, Ap&SS 276, 909
- Quinn, P. J., Hernquist, L., & Fullagar, D. P. 1993, ApJ, 403, 74
- Robertson, B., Bullock, J. S., Cox, T. J., Di Matteo, T., Hernquist, L. et al. 2006, ApJ, 645, 986
- Romeo, A. D., Napolitano, N. R., Covone, G., Sommer-Larsen, J., Antonuccio-Delogu, V. et al. 2008, MNRAS, 389, 13
- Semelin, B. & Combes, F. 2002, A&A, 388, 826
- Springel, V. & Hernquist, L. 2005, ApJ, 622, L9
- Velazquez, H. & White, S. D. M. 1999, MNRAS, 304, 254
- White, S. D. M. 1978, MNRAS, 184, 185
- White, S. D. M. 1979, MNRAS, 189, 831